IEEE Power Electronics Magazine, vol. 8, no. 2, pp. 24–33, 2021

Flexible and Efficient MMC Digital Twin Realized With Small-Scale Real-Time Simulators

S. Milovanovic, I. Polanco, M. Utvic, *et al.*

POWER ELECTRONICS LABORATORY
ÉCOLE POLYTECHNIQUE FÉDÉRALE DE LAUSANNE

Flexible and Efficient MMC Digital Twin Realized With Small-Scale Real-Time Simulators

by Stefan Milovanovic, Ignacio Polanco, Milan Utvic, and Drazen Dujic

The decreasing trend in the price of computational power has led to the evolution of various tools intended to support development processes in power electronics. In the domain of high-power converters, which rely on the use of digital controllers while switching at frequencies not exceeding several kHz, Hardware-In-the-Loop (HIL) systems have become widely adopted for commissioning and testing of control software. To put it differently, analog simulators or scaled-down versions of the same high-power converters have been replaced with HIL systems lately. Owing to the availability of computational power, HIL systems provide the means for high-fidelity real time simulations of the converter hardware parts. Connecting the dedicated controller, supposed to govern the hardware parts, to the Real-Time Simulator (RTS), through a suitable interface, gives control engineers the possibility to explore performances of various control algorithms without the controller ever realizing it drives the converter model, running on the employed RTS, instead of the real power hardware. Consequently, a risk-free environment for development and testing of control schemes is ensured, which is crucial especially if large and expensive systems, such as MW level power electronics converters, are considered. What is more, development of control algorithms and converter hardware parts can take place in parallel, as depicted in Figure 1, which reduces the development time of the converter as a whole.

Ensuring high fidelity of the real-time simulations requires inputs of the RTS to be read at high sampling rates. For example, capturing switching signals, provided by the controller, normally occurs at sampling times falling in the range of several nanoseconds, which guarantees accurate recognition of events crucial for the converter operation. Thereafter, the RTS uses information collected at its inputs to provide the outputs being as close as possible to the response observed in the real physical system. For that reason, the RTS is often regarded as the digital twin of the real power hardware. It is noteworthy that updating the RTS outputs occurs at fixed time steps, ranging from several hundreds of nanoseconds to several dozens of microseconds, depending on the way the simulator handles its calculations (in FPGA or CPU, respectively). However, realizing the digital twin of a system comprising a high number of switching devices imposes the need for an RTS with a high number of digital

Digital Object Identifier 10.1109/MPEL.2021.3075803
Date of current version: 16 June 2021

2329-9207/21©2021IEEE

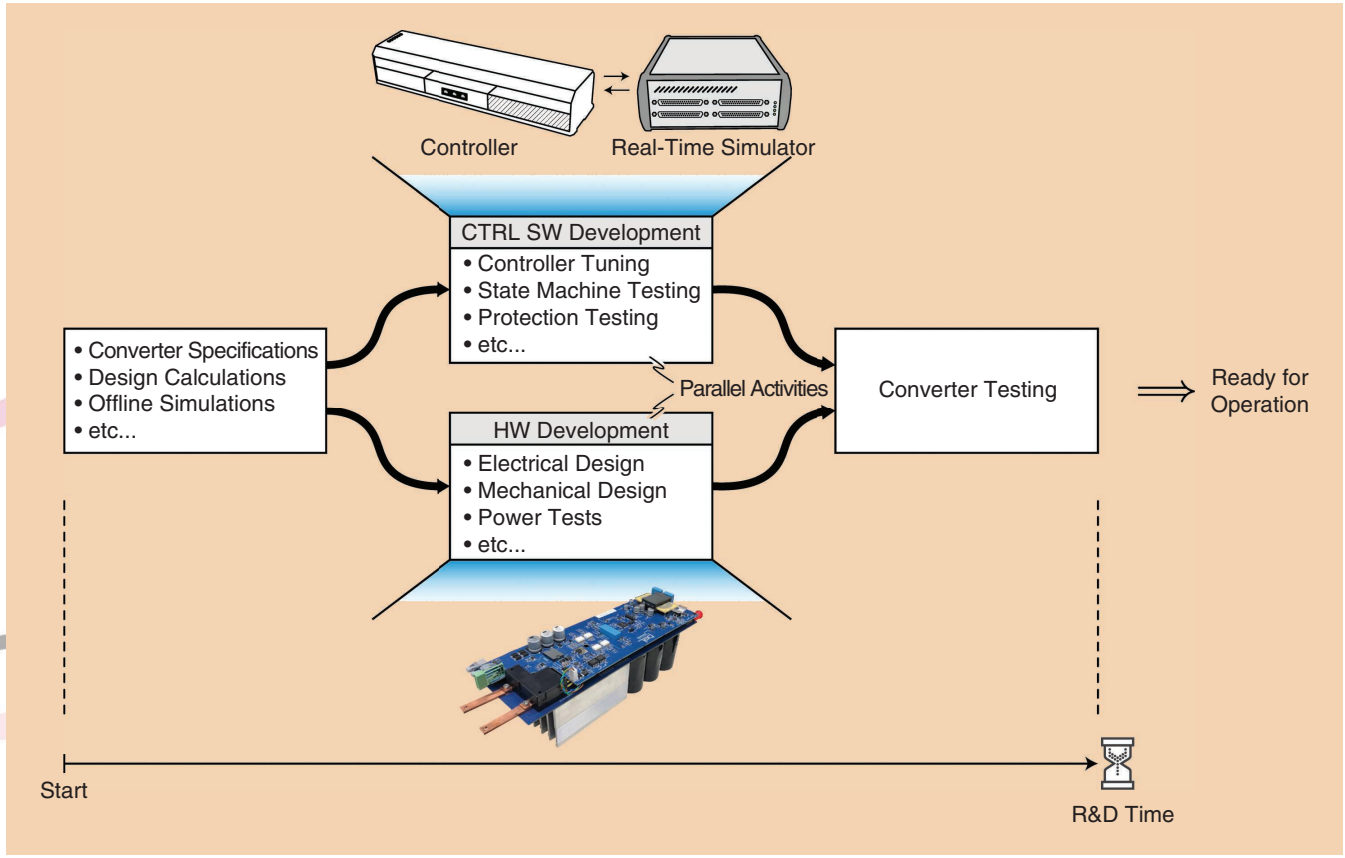

FIG 1 Technical steps in the realization of an arbitrary converter. An amenity provided by the HIL systems lies in the possibility to develop and test various control schemes simultaneously with the ongoing hardware design.

inputs (DIs), which might represent a challenge for small-scale HILs (e.g., Typhoon HIL, RT Box, SpeedGoat, StarSim, etc.). Such a technical hurdle can be circumvented through a suitable sectioning of the converter model allowing it to run on multiple HIL units, which is the subject being addressed in the following paragraphs. It should be stressed beforehand that large-scale simulators (e.g., RTDS, Opal RT, dSPACE), typically used in the power systems domain, also exist, however, this work relies on the use of their small-scale counterparts typically designed for power electronics applications.

This article describes how the digital twin of a system being as large as the Modular Multilevel Converter (MMC) [1], depicted in Figure 2, can be realized by means of the small-scale HIL units. Seven RT Box 1 [2] units, shown in Figure (3), were employed to run the model of a 3.3kVac/5kVdc, 250kVAr MMC comprising 48 full-bridge cells and operating in the rectifier mode. The developed digital twin was verified against an industrial ABB PEC800 controller, while all the steps in the system realization are supported by a thorough set of discussions, making the presented procedure extendable to other converters (e.g., Matrix MMC [3] or Δ-STATCOM [4]) used in the medium/high voltage domain.

MMC Modeling Suitable for Real-Time Simulations and the Need for Model Separation

As depicted in Figure 2, the MMC comprises a series connection of switching stages, referred to as the submodules (SMs) or cells. SMs are normally found in Half-Bridge (HB) or Full-Bridge (FB) configuration, while the other choices were listed in [5], [6]. A series connection of an SM cluster and an inductor is referred to as the branch, whereas two branches form the leg. By stacking the SMs in series, theoretically unlimited voltage scalability is provided while current capacity increase can be achieved in several ways, as already discussed in [7], [8]. Despite the above mentioned advantages, series connection of SMs comprises a high

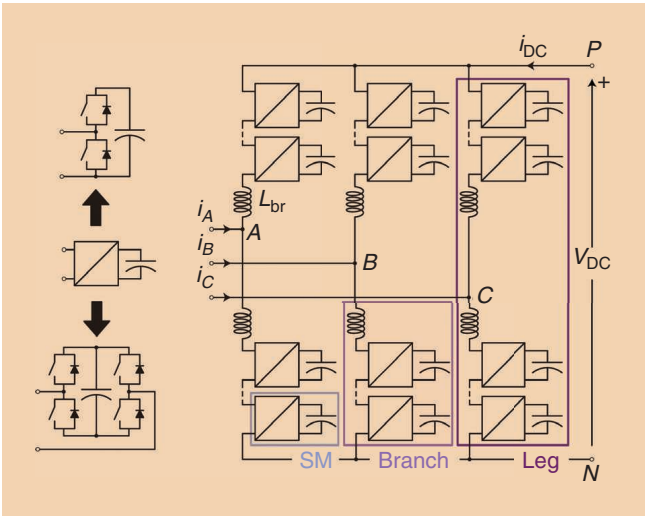

FIG 2 MMC and the adopted naming convention.

number of switching devices, making the MMC implementation challenging for any RTS.

Namely, in a system with a high number of switching devices, every combination of switches being on/off generates a unique system state. Recognizing and memorizing every state the system can be found in imposes tremendous computational burden upon the RTS. Therefore, minimization of switching elements, used to model an arbitrary converter, represents one of the key aspects in obtaining an efficient real time model.

Description	Number of Channels/Connectors	Voltage Range
Analog Inputs	16	–10 V ... 10 V
Analog Outputs	16	–10 V ... 10 V
Digital Inputs	32	3.3 V or 5 V
Digital Outputs	32	3.3 V or 5 V
SFP Ports	4	N.A.

FIG 3 PLECS RT Box 1 and its characteristics.

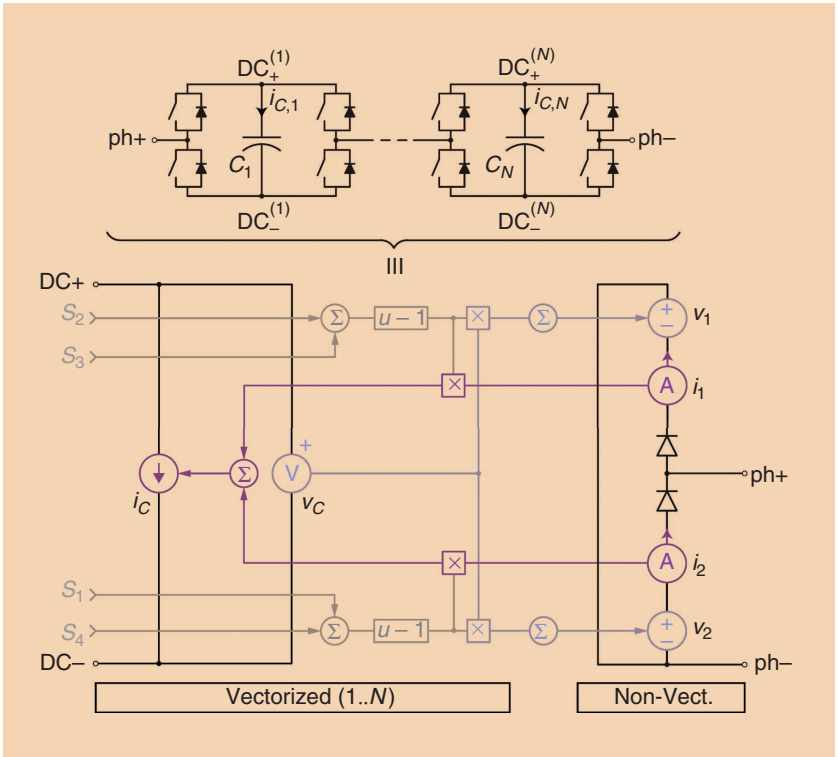

FIG 4 Branch model derived in [8]. Irrespective of the SM type (HB or FB), the branch model remains unchanged.

As presented in [9], a cluster of FB SMs can be modelled as in Figure 4, where controlled voltage sources v_1 and v_2 represent a combination of SM switching signals, provided by the controller and captured by the RTS, and instantaneous values of SM capacitor voltages, leading to the MMC model given in Figure 5. At its ac terminals, the MMC is interfaced with a three-phase voltage source through a series connection of an inductor and resistor. Thus, the same model can be used for real-time simulations of an MMC connected to an ac grid, ac machine or any other converter through the inductive interface (e.g., low-frequency transformer), making it general and extremely flexible.

Table 1 provides parameters of the grid-connected converter, operating in the rectifier mode, used for realization of the digital twin described hereafter. According to Table 1, the analyzed converter comprises $6 \times 8 = 48$ FB SMs, meaning that an RTS running the model from Figure 5 must be able to handle up to $48 \times 4 = 192$ switching signals, which far exceeds the 32 DIs available on the RT Box 1 presented in Figure 3 and referred to as HIL unit onwards. However, voltages v_1 and v_2 from Figure 4 can be calculated in an independent HIL unit for a branch comprising up to $32/4 = 8$ SMs. Conveniently, six independent HIL units can be used for calculation of relevant branch voltages, and these will be referred to as the Branch RT Boxes. Nonetheless, the model from Figure 5 needs to run on seventh HIL unit, being referred to as the Application RT Box, leading to the structure presented in Figure 6.

Owing to the insufficiency of the SFP ports on the Application RT Box rear panel, a daisy chain illustrated on the right-hand side of Figure 6 must be created. Moreover, one can notice the two types of boards interfaced with the Application and Branch RT Boxes, respectively, along with the so-called SM card. The need and derivation of the abovementioned components is addressed in the next section.

Detailed MMC HIL Description

It is straightforward to conclude from Figure 4 that calculation of branch voltage components v_1 and v_2 requires Branch RT Boxes to capture switching signals being delivered to the real physical SMs. Therefore, a certain interface between the Branch RT Box and the employed MMC controller must be ensured.

The SM being used as a reference point throughout the HIL realization process, and discussed in detail in [10], can be seen on the left-hand side of Figure 7. The developed MMC SM consists of two parts - power-board (the bottom one) and control-board (the top one). The control-board hosts all the logic (intelligence) related to the SM operation, which is an important detail in the digital twin development.

The goal of the developed HIL platform is to test different control schemes through virtual power processing. Hence, part of the SM processing the power can be modeled inside the RT Box, while the SM control-board needs to be retained and slightly adapted to the needs of the RTS. Namely, the control-board consists of several different parts, whose detailed description can be found in [10], however, adaptation allowing the real-time simulations requires only two of them.

First, every SM has its own Digital Signal Processor (DSP), controlling all the available SM functions (switching and protection signals, voltage/current measurements, etc.). Thus, the DSP is needed on the adjusted control-board. Second, communication with the MMC controller takes place through the Plastic Optical Fiber (POF) communication link. In the presented implementation, every SM receives its voltage and current reference, while providing the control system with information on its capacitor voltage, terminal current and general status, all through the POF RxTx pair. Consequently, the control-board of the real SM was re-organized with the aim of realizing the so-called HIL adjusted SM card, presented in Figure 7. As both adjusted and original control-board use the same connection to the employed controller, the controller is not able to differentiate between the HIL simulator and the real hardware prototype as long as the same DSP software is used in both cases. It is noteworthy that control-boards in their original form can also be used. Nevertheless, that approach, among other needs, requires an adequate power source supplying its Flyback converter, described in [11], with 650 V, making the structure in Figure 7 easier to use and design.

Based on the voltage reference received from the system controller, the SM creates its switching signals, which are subsequently read from the DSP pins by the IGBT module gate drivers. However, HIL implementation does not require parts such as gate drivers, therefore, DSP pins of the adjusted control board can be read directly from an RT Box including the IGBT module model. For that purpose, the interface board presented in Figure 7 was designed. As the use of FB modules is considered, four switching signals need to be supplied from the DSP to the RT Box for each one of the modeled SMs. In the opposite direction, SM terminal current and capacitor voltage measurements need to be communicated back to the DSP and subsequently to the controller employed in this work.

Figure 6 includes the Application RT Box, which is attached to its own Interface board. In general, parts of the real MMC controller (e.g., measurement interfaces) expect current/voltage signals to be adjusted to a certain range, which does not necessarily match the one provided by the RT Box. Apart from controlling the converter currents and voltages, the controller must monitor and control other auxiliary elements (e.g., breakers, relays, doors, fans, etc.), the behavior of which must also be emulated in the Application RT Box. Additionally, voltage signals (e.g., 24 V corresponding to logical 1) controlling the auxiliary elements might fall out of the range permitted by the RT Box (3.3V or 5 V). For that matter, Interface board was designed and employed as a simple intermediary stage between the RT Box and the MMC controller, as demonstrated in the next paragraphs.

As presented in Figure 8(a), the assembled system comprises seven RT Boxes. 48 SM HIL adjusted cards, hosting the DSP and logical circuitry of the real MMC SM described in [10], were interfaced with six Branch RT Boxes, each performing the calculation of voltage components relevant for an MMC branch. The seventh RT Box

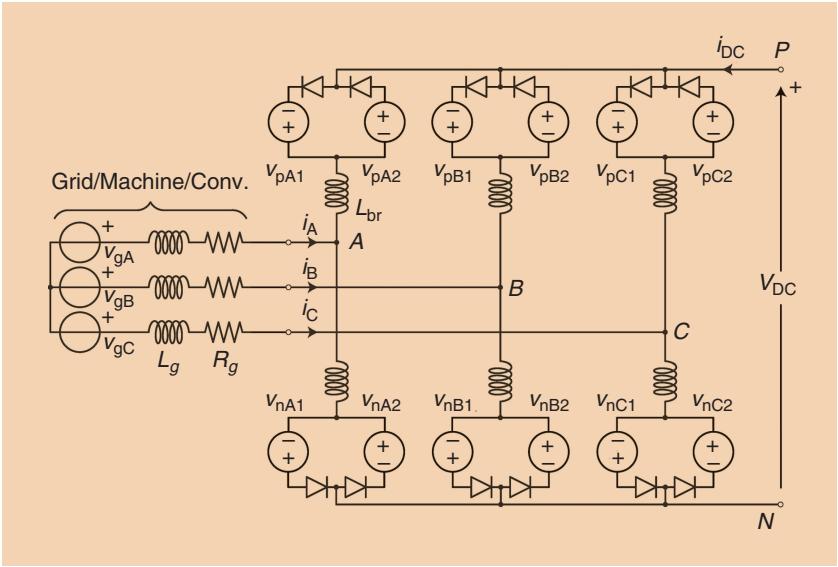

FIG 5 Real-time model of an MMC. Subscripts "p" and "n" denote upper and lower branch quantities, respectively.

Table 1. Rated Parameters of the simulated converter

Parameter	Label	Value
Rated power	S^*	250 kVAr
Output voltage	V_{DC}	5 kV
Grid voltage	v_g	3.3 kV
Number of SMs per branch	N	8
SM capacitance	C_{SM}	2.25 mF
Branch inductance	L_{br}	2.5 mH
Branch resistance	R_{br}	60 mΩ
PWM carrier frequency	f_{PWM}	1 kHz
Fundamental frequency	f_o	50 Hz
Grid inductance	L_g	13.86 mH

(fourth from the top in Figure 8(a)), contains the converter model provided in Figure 5.

In Figure 8(c), two ABB PEC800 controllers can be recognized and they are connected in the hierarchical structure. The main reason for such a configuration lies in the fact that several of these HIL systems can be connected to operate in various configurations. For example, control performance of multiple series connected MMCs, as mentioned in [12], [13], can be tested, while other options (e.g., back-to-back connection of two MMCs) are not excluded either. Each Slave controller is assigned the task of controlling its associated MMC, while one Master

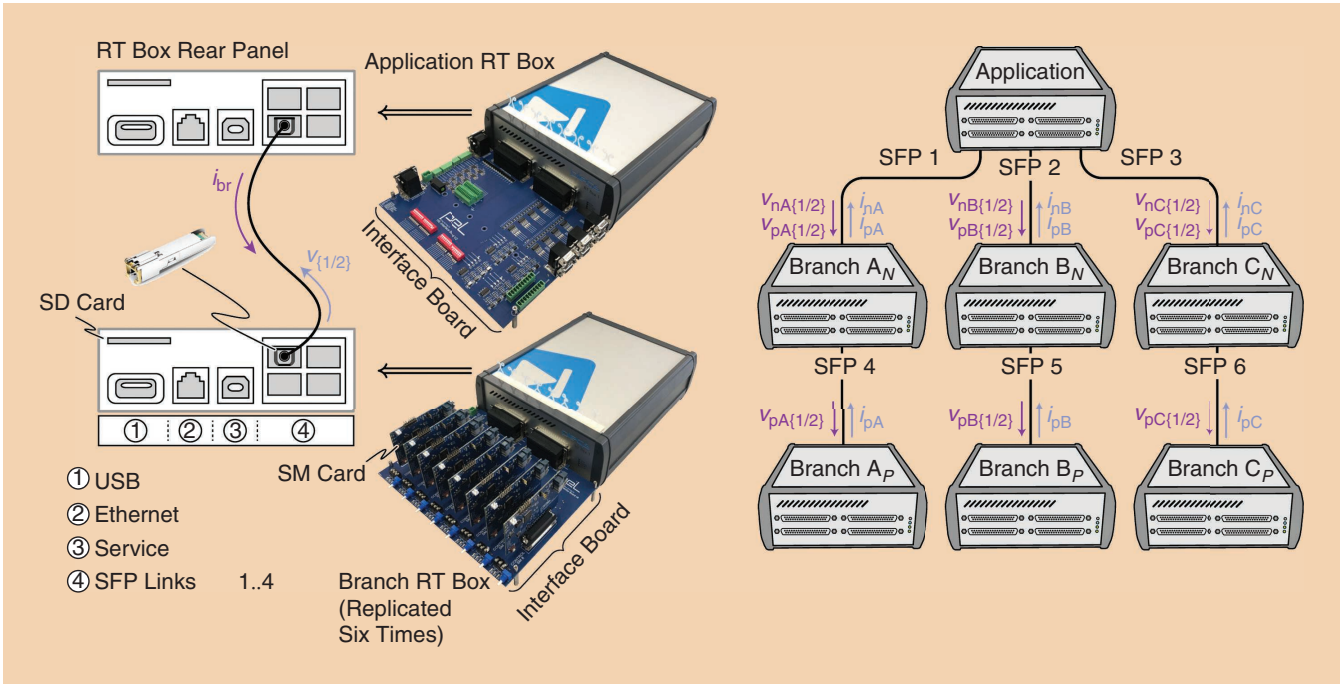

FIG 6 Two essential parts of the MMC RTS realized by means of RT Boxes. By means of the SFP links, Branch RT Boxes provide the Application RT Box with voltage components labeled with v1 and v2 in the adopted branch model. On the other hand, information on a relevant branch current is sent back to the Branch RT Box, which is needed according to [[8]].

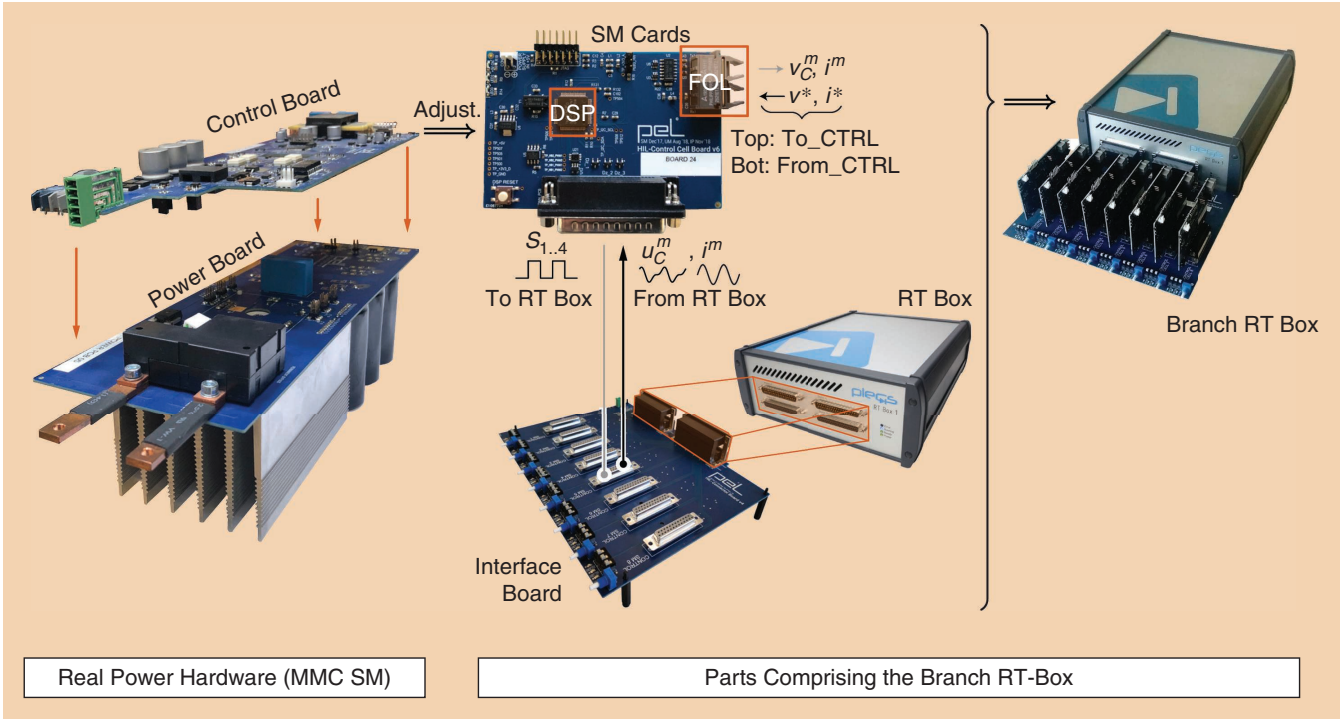

FIG 7 On the left, one can see the SM design being followed in the HIL system development (power-board + control-board). Power part of the MMC SM is modeled inside the RTS, while control-board of the SM is adjusted such that used controller cannot observe any difference between the developed simulator and a real hardware prototype. As DSP pins of the adjusted control-board cannot be read directly by an RT Box, an interface board was designed.

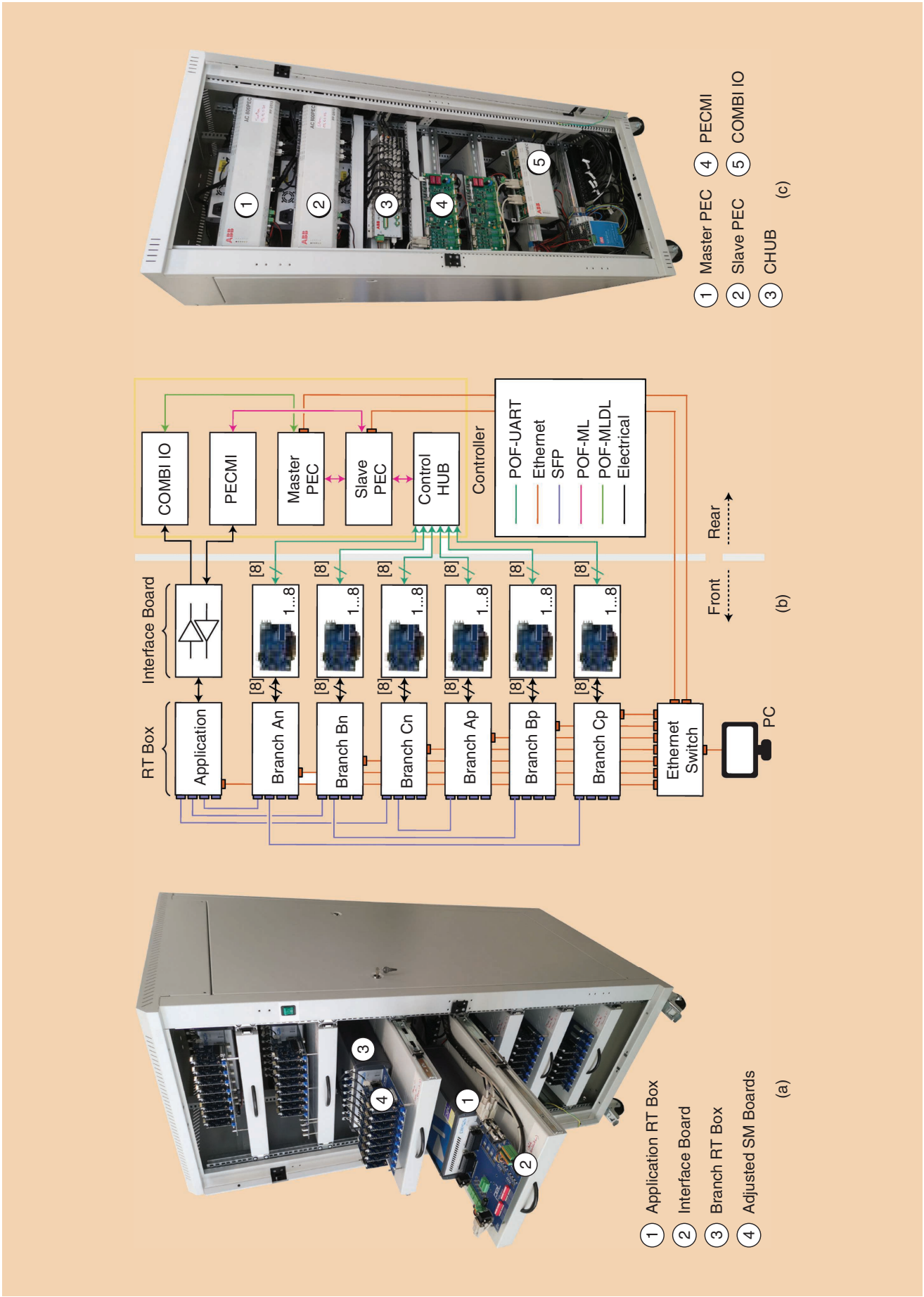

FIG 8 Assembled HIL system: (a) Front view; (b) Wiring diagram; (c) Rear view.

controller is to handle general (application) state machine and references. Other parts of the system, visible in Figure 8(c), are in charge of voltage/current measurements (PECMI), distribution of SM optical signals (CHUB) and manipulation of relays, switches and other user defined arbitrary signals (COMBIO). Real MMC prototype uses the identical control structure, making the presented HIL indeed reliable from the control test/verification viewpoint.

Figure 8(b) provides the wiring diagram of the system. As can be seen, communication between the PC and other system parts is established through an Ethernet switch. SM-cards communicate with the control system through POF pair, whereas conventional UART protocol is used for this purpose. Also, communication among different controller parts happens through POF links, however, a different ABB proprietary protocol named MultiLink (labeled with ML) is relied on. Connection between two (or multiple) RT Boxes can be established through the SFP ports. However, one RT Box contains four SFP links, leading to the conclusion that six Branch RT Boxes cannot be directly connected to the Application RT Box. Therefore, daisy chain presented in Figure 8(c) had to be created.

Connecting the dedicated controller, supposed to govern the hardware parts, to the Real-Time Simulator (RTS), through a suitable interface, gives control engineers the possibility to explore performances of various control algorithms without the controller ever realizing it drives the converter model, running on the employed RTS, instead of the real power hardware.

Real-Time Simulation Results

Results presented hereafter were obtained on the model of the converter, operating in the rectifier mode, with parameters already provided in Table 1. Distribution of the MMC model over seven RT Boxes was performed; however, computational burden imposed on Branch and Application RT Boxes was not the same. Therefore, real time simulation step sizes were selected differently as $T_{\text{step}}^{\text{app}} = 7\mu\text{s}$ and $T_{\text{step}}^{\text{br}} = 3.5\ \mu\text{s}$. Functionality of the assembled device was conducted based on different operating regimes described below.

1) MMC Charging

Figure 9 reveals several stages in the converter charging process. One can see that all quantities are equal to zero as long as no voltage is present on the grid side. Such a situation describes the converter being disconnected from the grid and it was labeled with ①. Immediately upon connecting the MMC to the ac grid, voltages v_{gA}, v_{gB} and v_{gC} become different than zero and this time instant implies the beginning of passive charging process, labeled with ②.

Once the passive charging commences, grid currents i_{gA}, i_{gB} and i_{gC} start to flow toward the MMC. Since SM capacitors are not charged, a set of charging resistors, the model of which is irrelevant for the scope of this article, limits the inrush current from the grid. As voltage across SM capacitors builds up, magnitude of grid currents decays according to the exponential law, given that the observed circuit features *RC* nature. Bypassing of charging resistors designates the end of the charging process. During passive charging, every branch behaves as a single-phase diode rectifier. Consequently, branches get charged to the level matching the amplitude of the grid phase voltage. In this way the converter is not necessarily fully charged to match its application operating point. Nevertheless, the ac grid currents can be controlled, therefore, further voltage boost can be performed through the so-called active charging process. Between passive and active charging processes there is a certain period referred to as the timeout, and it was labeled with ③. As every branch features a diode rectifier nature, SM capacitors cannot get discharged back to the grid, which can be seen in the plot presenting the total branch voltages (the first plot from the bottom).

When the active charging process, labeled with ④, commences, branches start to switch, which can be observed from the plot presenting instantaneous values of voltage components $v_{\text{pA1}}, v_{\text{pA2}}, v_{\text{nA1}}$ and v_{nA2}. As relevant voltage components in legs *B* and *C* are shifted by one third of the fundamental period, they are not presented. During active charging, AC grid currents are controlled such that the converter internal energy increases, which is equivalent to total branch voltages increasing to the setpoint value (5 kV). Once the converter gets charged, the active charging is considered over and the controller state machine brings the converter into the operating state, which is labeled with ⑤. At this point, the converter can create an arbitrary DC voltage falling in the range of –5 kV…5 kV. However, in the example discussed so far, $V_{\text{DC}}^{*} = 0$ for simplicity reasons.

2) No Load Operation

To prove that the demonstrated modeling approach can be used in case the converter branches receive switching signals, no load operation is presented in Figure 10. To control the grid currents, branches receive voltage references being realized through the PWM gate signals.

As the number of SMs per branch equals $N_{SM} = 8$, every branch creates up to $N_{SM} + 1 = 9$ voltage levels, which is straightforward to confirm from Figure 10. Further, as no power is processed to the dc side, the converter total energy balancing requires almost no current to be drawn from the ac side. However, balancing of the SM voltages, in case phase shifted carrier (PSC) modulation is used, requires the presence of currents circulating inside of the converter. In this work, circulating currents at double the fundamental frequency and with amplitude equal to 20 A were used. Lastly, dc voltage and

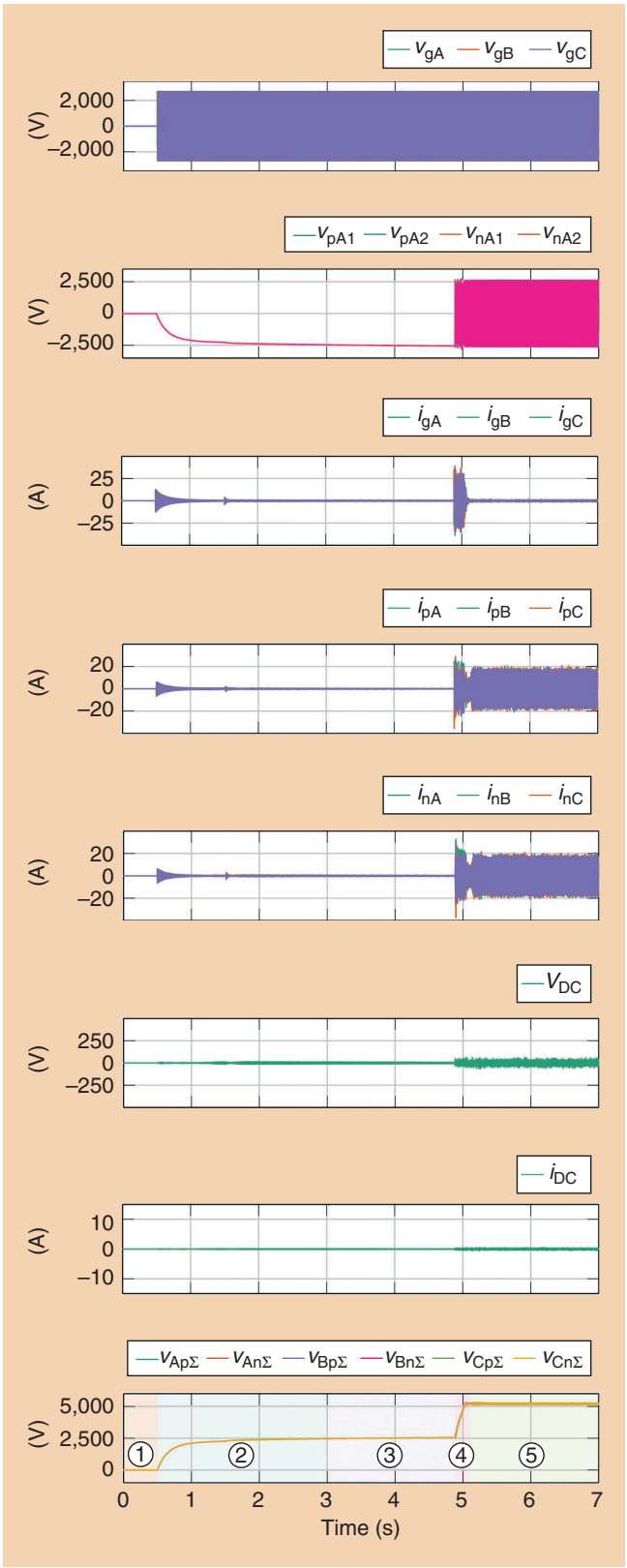

FIG 9 Converter charging process presented through several stages.

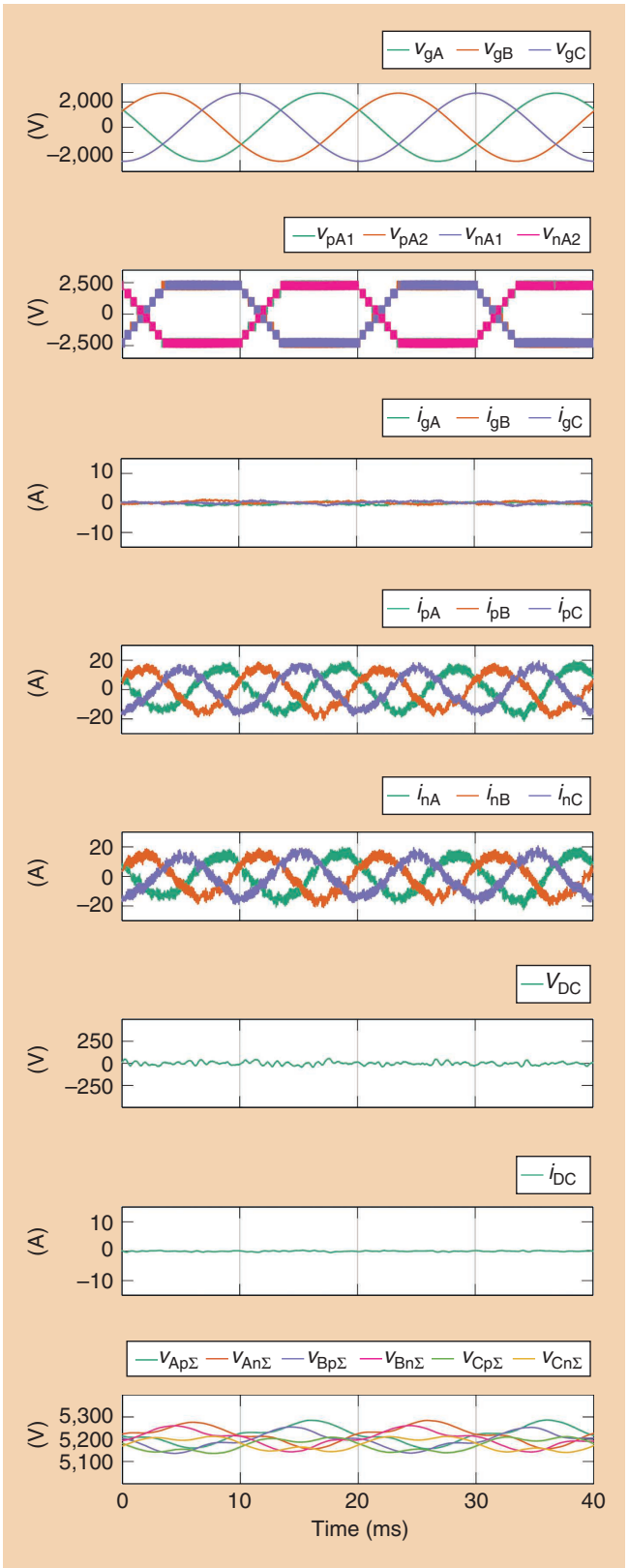

FIG 10 No load operation ($P_{DC} = 0$).

current average values equal zero, whereas a certain amount of ripple, being caused by the switching, cannot be avoided.

3) Operation at Full Load

Figure 11 presents the converter operating waveforms in case energy is transferred from AC to DC side (rectifier mode) at nominal power. As the grid currents increase in amplitude so do the branch currents, which in conjunction with branch voltages causes branch powers, and inherently voltages, to oscillate. Similar to the case considering operation at no load, dc voltage and current contain the switching ripple, however, with mean values being different

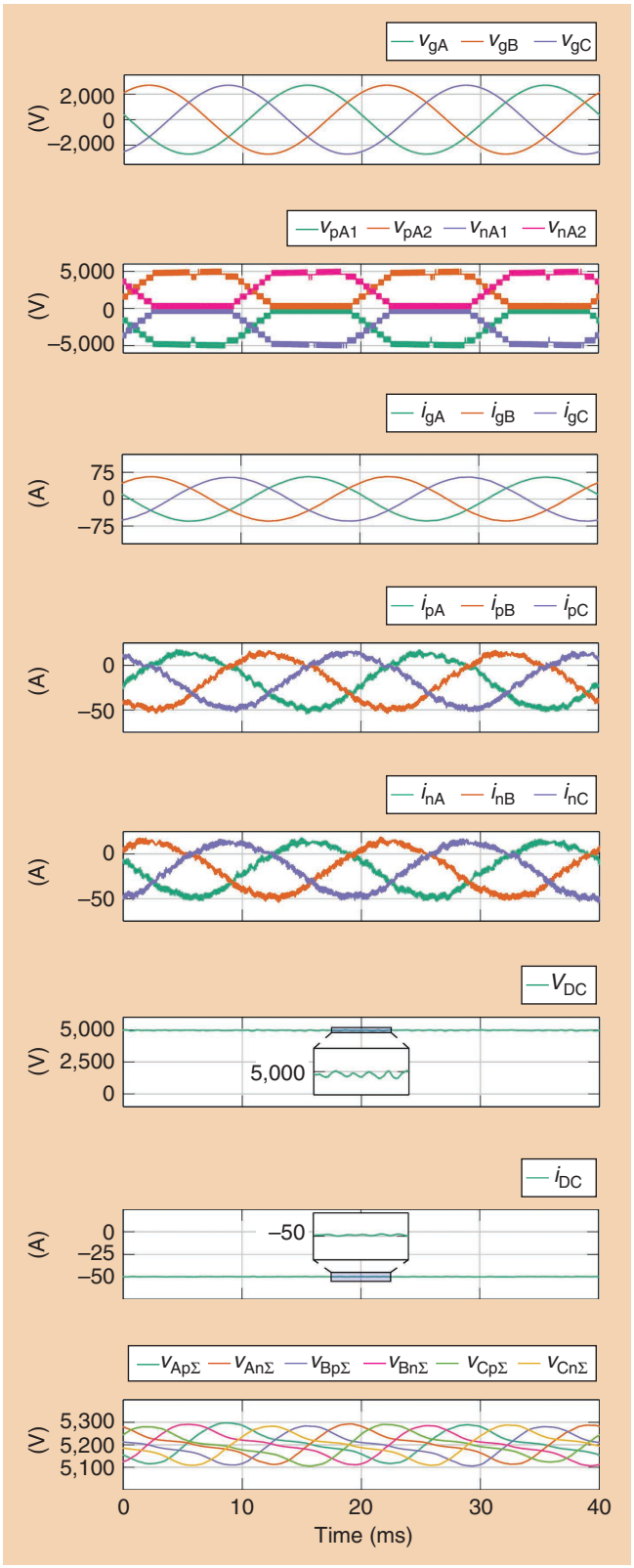

FIG 11 Full-load operation ($P_{DC} = 250$ *kW*).

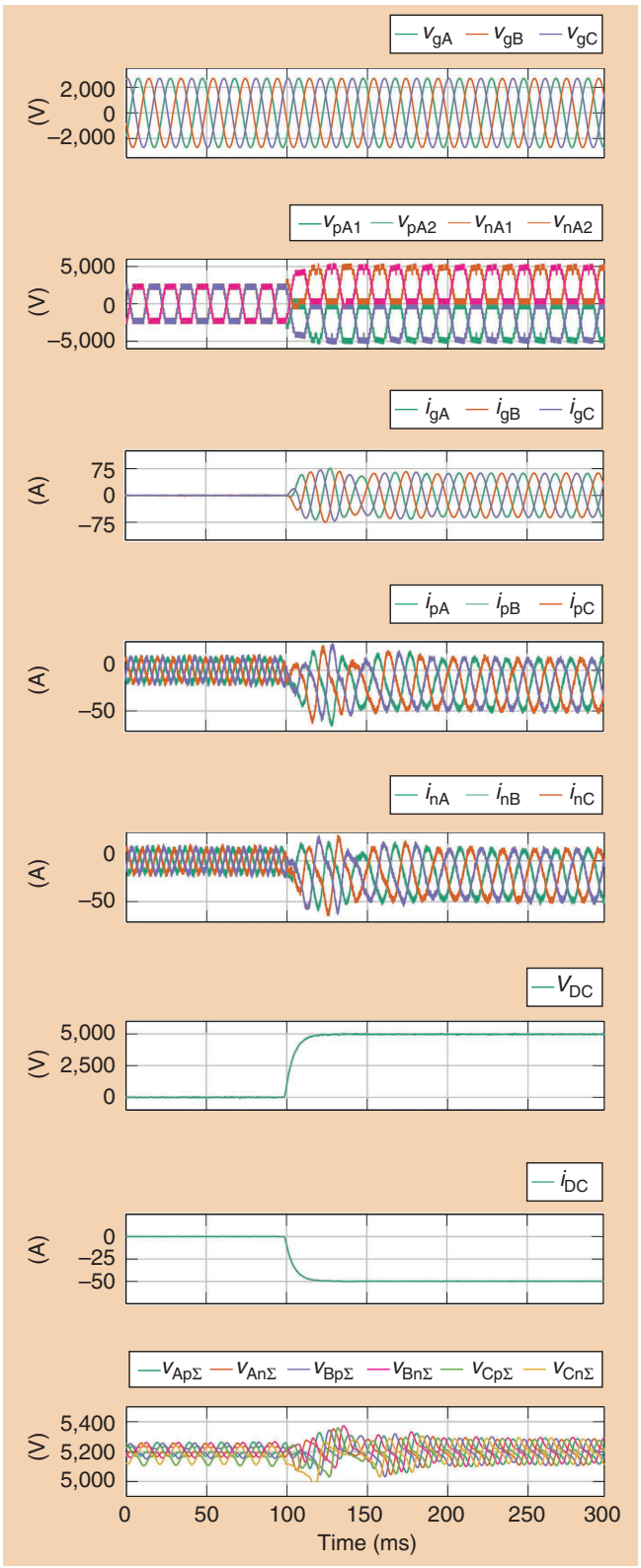

FIG 12 Operating waveforms in case dc voltage reference is changed from 0 to 5 kV.

than zero. As can be seen, tracking of the dc voltage, labeled with V_{DC}, with a negligible error was achieved, while negative value of the dc current originates from the adopted reference direction. Lastly, branch currents contain an offset equal to one third of the dc current and half of the ac current associated with an observed converter leg.

4) Voltage Reference Change

Figure 12 presents the converter operating waveforms in case dc voltage reference is changed from 0 to 5 kV. To avoid fast discharge of the SM capacitors, a first-order filter, with the time constant $\tau = 10$ ms, was applied to the dc voltage reference.

Careful inspection of test scenarios provided above reveals that the presented waveforms correspond to their theoretical shapes, leading to the conclusion that the assembled HIL system indeed provides a realistic and flexible environment for testing of various MMC control schemes. In the above paragraphs, test results obtained on a single HIL simulator were presented, however, controller structure allows for a simultaneous operation of up to four systems presented in Figure 8. More discussions on this subject can be found in [12].

Conclusion

This article provided an extensive description of the MMC digital twin realized by means of the small-scale HIL units (i.e., RT Boxes). The MMC model, suitable for real-time simulations, was sectioned and distributed over seven RT Boxes, demonstrating flexibility and scalability of this real-time simulation platform. Validation of the assembled system was performed by means of an industrial ABB PEC800 controller equipped with additional elements (currents/voltages measurements (PECMI), boards governing relays/breakers (COMBIO), etc.) normally used in real hardware implementations. Therefore, the presented platform can be considered reliable from the viewpoint of MMC control testing, which outlines the potential of small-scale HILs in realization of systems utilizing multiple switching elements, such as the MMC.

Acknowledgment

This work has received funding, in part from the European Union's Horizon 2020 research and innovation program under Grant Agreement No 881772 (FUNDRES project), and in part from the Swiss Innovation Agency - Innosuisse, as the innovation project 38041.1 IP-ENG.

About the Authors

Stefan Milovanovic (stefan.milovanovic@epfl.ch) is a postdoctoral researcher in the Power Electronics Laboratory at Ecole Polytechnique Fédérale de Lausanne, Switzerland. His research is focused on medium/high voltage high power conversion.

Ignacio Polanco is a Ph.D. student at Power Electronics Laboratory at Ecole Polytechnique Fédérale de Lausanne, Switzerland. His Ph.D. research work is related to condition health monitoring of modular converter systems.

Milan Utvic is a Ph.D. student at Power Electronics Laboratory at Ecole Polytechnique Fédérale de Lausanne, Switzerland. His Ph.D. research work is related to robust control for high power converter systems.

Drazen Dujic (drazen.dujic@epfl.ch) is an associate professor and head of Power Electronics Laboratory at Ecole Polytechnique Fédérale de Lausanne, Switzerland. His research interests are predominantly related to high power conversion technologies for medium voltage applications.

References

[1] A. Lesnicar and R. Marquardt, "An innovative modular multilevel converter topology suitable for a wide power range," *2003 IEEE Bol. PowerTech - Conf. Proc*, vol. 3, pp. 272–277, 2003. doi: 10.1109/PTC.2003.1304403.

[2] "RT box manual," Plexim GmbH, https://www.plexim.com/sites/default/files/rtboxmanual.pdf

[3] F. Kammerer, M. Gommeringer, J. Kolb, and M. Braun, "Energy balancing of the modular multilevel matrix converter based on a new transformed arm power analysis," in *Proc. 16th Eur. Conf. Power Electron. Appl. EPE-ECCE Eur.*, 2014. doi: 10.1109/EPE.2014.6910939.

[4] F. Z. Peng and J. Wang, "A universal STATCOM with delta-connected cascade multilevel inverter," *PESC Rec. – IEEE Annu. Power Electron. Spec. Conf*, vol. 5, pp. 3529–3533, 2004. doi: 10.1109/PESC.2004.1355099.

[5] A. Nami, J. Liang, F. Dijkhuizen, and G. D. Demetriades, "Modular multilevel converters for HVDC applications: Review on converter cells and functionalities," *IEEE Trans. Power Electron.*, vol. 30, no. 1, pp. 18–36, 2015. doi: 10.1109/TPEL.2014.2327641.

[6] S. Heinig, "Main circuits, submodules, and auxiliary power concepts for converters in HVDC grids," KTH PhD thesis, 2020.

[7] S. Milovanovic and D. Dujic, "On facilitating the modular multilevel converter power scalability through branch paralleling," in *Proc. IEEE Energy Convers. Congr. Expo*, 2019, pp. 6875–6882.

[8] S. Milovanovic and D. Dujic, "On power scalability of modular multilevel converters: Increasing current ratings through branch paralleling," *IEEE Power Electron. Mag.*, vol. 7, no. 2, pp. 53–63, 2020. doi: 10.1109/MPEL.2020.2984350.

[9] J. Allmeling and N. Felderer, "Sub-cycle average models with integrated diodes for real-time simulation of power converters," in *Proc. IEEE South. Power Electron. Conf. SPEC 2017*, 2018. doi: 10.1109/SPEC.2017.8333566.

[10] M. Utvic, I. P. Lobos, and D. Dujic, "Low voltage modular multilevel converter submodule for medium voltage applications," in *Proc. PCIM Eur. 2019; Int. Exhib. Conf. Power Electron. Intell. Motion, Renew. Energy Energy Manag.*, 2019, pp. 1–8.

[11] A. Christe, M. Petkovic, I. Polanco Lobos, M. Utvic, and D. Dujic, "Auxiliary submodule power supply for a medium voltage modular multilevel converter," *CPSS Trans. Power Electron. Appl.*, vol. 4, no. 3, pp. 204–218, 2019. doi: 10.24295/CPSSTPEA.2019.00020.

[12] M. M. Steurer et al., "Multifunctional megawatt-scale medium voltage DC test bed based on modular multilevel converter technology," *IEEE Trans. Transp. Electrif.*, vol. 2, no. 4, pp. 597–606, 2016. doi: 10.1109/TTE.2016.2582561.

[13] M. Utvic and S. Milovanovic, "Flexible medium voltage DC source utilizing series connected modular multilevel converters," in *Proc. 21st Eur. Conf. Power Electron. Appl. EPE 2019 ECCE Eur*, 2019, pp. 1–9. doi: 10.23919/EPE.2019.8915466.

PEM